Multi-Wavelength Fiber Ring Laser Based on Mach-Zehnder Interferometer of Dispersion Compensation Fiber Connection Point

Wang Jishun[1,2] Yu Yongqin[2,3] Ou Zhilong[1,2] Huang Quandong[1,2] Chen Xue[1,2]
Yan Peiguang[1,2] Du Chenlin[1,2]

([1] *College of Electronic Science and Technology, Shenzhen University, Shenzhen, Guangdong* 518060, *China*
[2] *Shenzhen Key Laboratory of Laser Engineering, Shenzhen, Guangdong* 518060, *China*
[3] *College of Physics Science and Technology, Shenzhen University, Shenzhen, Guangdong* 518060, *China*)

Abstract Stable multi-wavelength lasing based on in-fiber Mach-Zehnder interferometer (MZI) introduced by dispersion compensation fiber (DCF) in an erbium-doped fiber ring laser is presented. This interference effect effectively suppresses the unstable mode competition caused by homogeneous line broadening which leads to the generation of stable multi-wavelength lasing at room temperature. The dual-wavelength lasing is so stable and the peak fluctuation is less than about 1.1 dB, while the peak fluctuation of the tri-wavelength lasing is much larger with a value of about 4 dB.

Key words fiber optics; lasers; finite element method; dispersion compensation fiber
OCIS codes 060.2310; 060.4510; 060.2280; 140.3500

基于色散补偿光纤马赫-曾德尔干涉的多波长光纤环形激光器

王继顺[1,2] 于永芹[2,3] 欧志龙[1,2] 黄权东[1,2] 陈 雪[1,2] 闫培光[1,2] 杜晨林[1,2]

([1]深圳大学电子科学与技术学院，广东 深圳 518060；[2]深圳激光工程重点实验室，广东 深圳 518060
[3]深圳大学物理科学与技术学院，广东 深圳 518060)

摘要 报道了一种基于色散补偿光纤内的马赫-曾德干涉效应的掺铒光纤环形激光器，得到了稳定的多波长激光输出。这种干涉效应有效地抑制了由均匀谱线展宽效应引起的不稳定的模式竞争，从而在室温下能够得到稳定的多波长激光输出。双波长激光输出比较稳定，峰值波动约小于 1.1 dB，而三波长激光输出的峰值波动约为 4 dB。

关键词 光纤；激光器；有限元法；色散补偿光纤
中图分类号 TN248 **文献标识码** A **doi**：10.3788/CJL201441.s105002

1 Introduction

Multi-wavelength erbium-doped fiber lasers are focused on research in stable spectrum width and narrower lasing line width due to their potential applications in diverse fields including wavelength division multiplexed (WDM) fiber-communication systems, precise spectroscopy, optical fiber sensors, filter, and optical instrument testing[1-8].

To realize multi-wavelength oscillations at room temperature, the unstable mode competition induced by the homogeneous line broadening and cross-gain saturation of erbium-doped fiber (EDF) must be suppressed. Polarization hole burning (PHB) effect[5], or nonlinear effects such as stimulated Brillouin scattering[9-10] and four-wave mixing[11-13] into the laser cavity have been proposed. In addition, stable multi-

收稿日期：2013-10-07；**收到修改稿日期**：2013-11-13
基金项目：国家自然科学基金(61275125, 61007054, 61308055)、深圳市科技计划项目(JC201005280473A, JC201104210019A, ZDSY20120612094753264, JCYJ20130326113421781)、教育部博士学科点专项科研基金(20124408120004)
作者简介：王继顺(1989—)，男，硕士研究生，主要从事光纤激光器方面的研究。E-mail：wangjishun@email.szu.edu.cn
导师简介：于永芹(1976—)，女，博士，副教授，主要从事光子晶体光纤非线性、光纤光栅及光纤传感器等方面的研究。E-mail：yuyq@szu.edu.cn(中国光学学会会员号：8042011610S)

wavelength lasing can be obtained based on Mach-Zehnder interferometer (MZI)[14-17]. A dual-pass MZI fiber device is used as a comb filter inside the laser cavity. To achieve simultaneous multi-wavelength lasing, the erbium-doped fiber was immersed in liquid nitrogen (at a temperature of 77 K) to reduce the homogeneous line width to 1 nm[14]. Although the experiment can operate at room temperature, it has a relatively complex formation[15].

In this paper, the L-band multi-wavelength generation of fiber ring laser using dispersion compensation fiber (DCF) based on MZI is presented. Own to introducing the DCF into the laser cavity, we can obtain stable multi-wavelength lasing at room temperature. By increasing the pump power and adjusting the polarization controller (PC), a different number of stable multi-wavelength lasing lines can be obtained.

2 Device fabrication and theoretical analysis

The diameters of core and cladding of the DCF are 4 μm and 125 μm, respectively. The refractive indices of core and cladding are 1.473 and 1.445, respectively. The propagation mode properties of the DCF are analysed by finite element method (FEM, COMSOL 3.5a). The DCF used in our experiment can guide the modes of LP_{01} and LP_{02} at wavelength range from 1520 nm to 1600 nm. Figure 1 shows the effective mode refractive indices as a function of wavelengths from 1520 nm to 1600 nm and the insets are the calculated mode field distribution of LP_{01} (left) and LP_{02} (right) by FEM at wavelength of 1590 nm. The effective mode refractive indices of LP_{01} and LP_{02} at wavelength of 1590 nm are 1.46776 and 1.46001, respectively. Therefore, the refractive indices difference Δn_{eff} is 0.00775.

Figure 2 presents a schematic of the SMF-DCF-SMF MZI constructed by two ends of a DCF splicing with single mode fibers (SMFs) using a commercial fusion splicer (Fujikura, FSM-60S). The core diameter of SMF is 8.5 μm. Due to the mode mismatch between the DCF and SMF, the insertion loss of DCF is about 1.93 dB in the experiment.

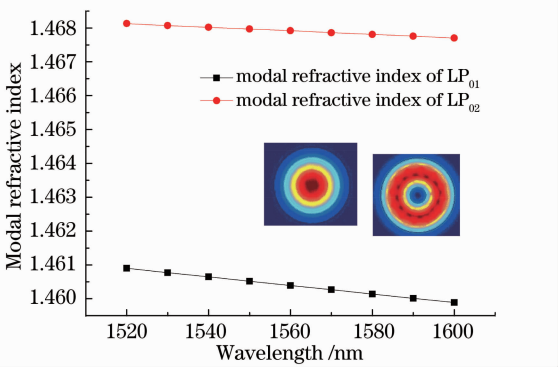

Fig. 1 Modal refractive indices of LP_{01} and LP_{02} versus wavelength. Inset are the calculated mode field distributions of LP_{01} (left) and LP_{02} (right) by FEM

Fig. 2 Schematic of the SMF-DCF-SMF MZI

In Fig. 2, when the light through the SMF reaches at first spliced point, high order modes in the core of DCF are motivated. The phase difference of different modes dependes on the wavelength and the length of DCF is produced because of their different effective indices. When the guided light in DCF arrives the second spliced point, the excited different modes are re-coupled back to the fundamental mode of SMF and cause the generation of interference due to the phase difference. The two spliced points act as couplers of dividing or combining light powers in the arms of the interferometer. In order to prove that stable multi-wavelength lasing is obtained based on the MZI introduced by DCF, rather than the influence of other factors, an experiment is made to obtain the MZI by using different lengths of DCF. Figure 3 shows the experimental setup which is formed by an amplified spontaneons emission (ASE) light source (C + L band, LIGHTCOMM) and the transmission spectrum is monitored by an optical spectra analyzer (OSA, yokogawa, AQ6370B). The MZI spectra corresponding to different lengths of DCF are shown in Fig. 4. The interference patterns are not perfectly sinusoidal for different intensities of the interferential modes. We can see that the phenomenon of MZI becomes obvious and the fringe spacing $\Delta\lambda$ becomes smaller as the length of DCF increases. Shorter length of DCF is helpful to obtain larger fringe spacing. The total intensity of the MZI spectrum can be expressed as

$$I(\lambda) = I_1(\lambda) + I_2(\lambda) + 2\sqrt{I_1(\lambda) I_2(\lambda)}\cos(2\pi\Delta n_{\text{eff}} L/\lambda), \quad (1)$$

where $I_1(\lambda)$ and $I_2(\lambda)$ are the intensities of the two interferential modes at wavelength of λ. L is the length of MZI. Δn_{eff} is the effective indices difference of two modes. $\varphi = 2\pi\Delta n_{\text{eff}} L/\lambda$ is the phase difference of two modes, and it is dependent on wavelength. Transmission dips appear when phase matching is satisfied with

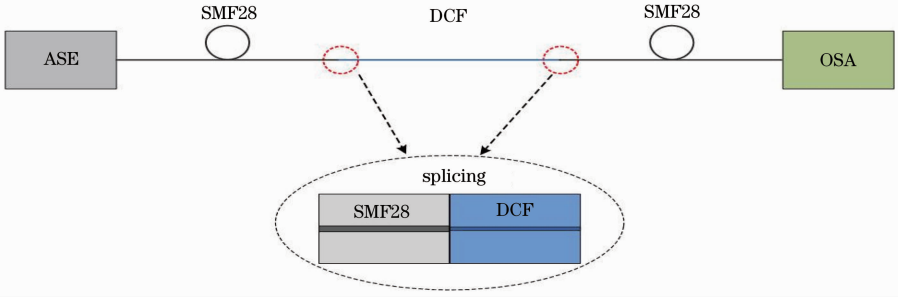

Fig. 3 Experimental setup of MZI

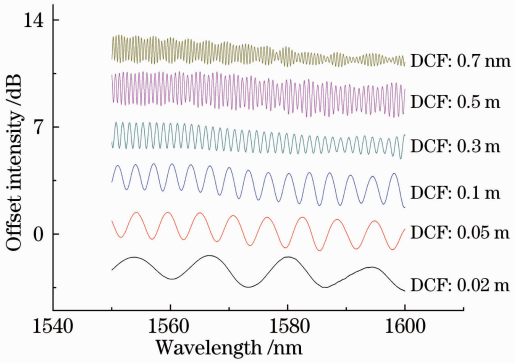

Fig. 4 MZI spectra corresponding to different lengths of DCF

$$\varphi = 2\pi\Delta n_{\text{eff}} L/\lambda = 2\pi(n_{\text{eff}}^{\text{core}} - n_{\text{eff}}^{\text{HOM}})L/\lambda = (2k+1)\pi. \quad (2)$$

where k is a positive integer; $n_{\text{eff}}^{\text{core}}$, $n_{\text{eff}}^{\text{HOM}}$ represent the effective mode refractive indices of the fundamental mode and the high order mode, respectively. From the phase matching condition, the fringe spacing $\Delta\lambda$ of the MZI spectrum can be expressed as

$$\Delta\lambda = \lambda^2/(\Delta n_{\text{eff}} L). \quad (3)$$

It indicates that the fringe spacing $\Delta\lambda$ is in inverse proportion to the length L of MZI, which is consistent with the experimental results.

Figure 5 shows the MZI spectrum caused by the DCF of 0.7 m. The fringe spacing $\Delta\lambda$ is obtained to be 0.5 nm at wavelength of 1590 nm. Via Eq. (3) and the MZI spectra in the experiment, the effective indices difference Δn_{eff} of LP_{01} and LP_{02} can be calculated and table 1 shows the effective indices difference from 1520 nm to 1600 nm calculated by FEM and Eq. (3), respectively. It shows that the result calculated by FEM matches well with the experimental result which indicates that the interference fringe is caused by LP_{01} and LP_{02} modes interference.

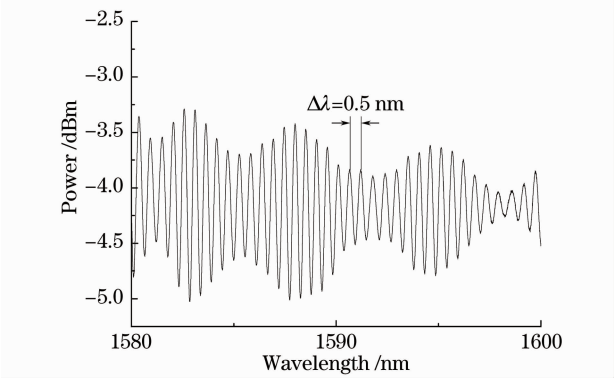

Fig. 5 MZI spectrum caused by the DCF of 0.7 m

Table 1 Effective indices difference between LP_{01} and LP_{02}

Wavelength /nm	$\Delta\lambda$ /nm	Refractive indice of LP_{01}	Refractive indice of LP_{02}	Δn_{eff} (FEM)	Δn_{eff} (experiment)
1520	0.46	1.46813	1.4609	0.00723	0.00717
1530	0.464	1.46807	1.46077	0.0073	0.00721
1540	0.468	1.46802	1.46065	0.00737	0.00724
1550	0.48	1.46797	1.46052	0.00745	0.00715
1560	0.484	1.46792	1.46039	0.00753	0.00719
1570	0.492	1.46786	1.46027	0.00759	0.00716
1580	0.496	1.46781	1.46014	0.00767	0.00719
1590	0.5	1.46776	1.46001	0.00775	0.00723
1600	0.512	1.4677	1.45989	0.00781	0.00714

3 Experimental setup

Figure 6 is schematic diagram of the experimental setup. A highly-doped erbium doped fiber (EDF) is employed to provide broadband gain for the generation of L-band multi-wavelength lasing. The absorption coefficient in the erbium-doped fiber at 1.53 μm is about 80 dB/m. A 980 nm laser diode (LD) is used for pumping the EDF with length of 1.5 m through a wavelength

division multiplexing (WDM) coupler. A PC is employed to adjust and match the state of polarization of the propagating light. An optical isolator (ISO) is used for the unidirectional operation of the ring laser. A 10/90 coupler is inserted to extract 10% coupling output of the laser monitored by the OSA while the remaining 90% radiation is incident to laser cavity. The DCF-MZI is the most important component for the generation of multi-wavelength oscillation. When the fundamental mode that propagates along the SMF couples into the DCF, it will excite different interference modes at the SMF-DCF splice point due to the large core diameter mismatch[18] and generate the interference pattern. Thus it results in the different distributions of gain and loss along the laser cavity at different wavelengths and finally suppresses the unstable mode competition caused by homogeneous line broadening which leads to the generation of multi-wavelength lasing.

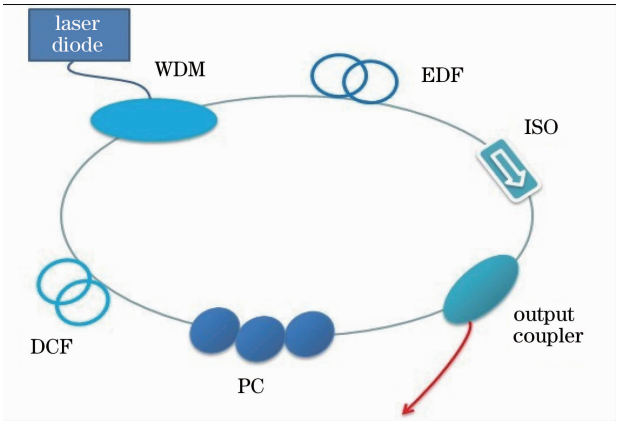

Fig. 6 Schematic diagram of experimental setup

4 Results and discussion

DCFs with lengths of 0.1 m and 0.7 m are used to be put respectively into the laser cavity and stable multi-wavelength lasing is obtained. Figure 7 shows the MZI spectrum caused by the DCF of 0.1 m and the corresponding laser output spectrum. It can be seen that the fringe spacings ($\Delta\lambda$) of the MZI spectrum and the laser output spectrum are equal to each other with the value of 3.48 nm. Figure 8 shows the MZI spectrum caused by the DCF of 0.7 m and the laser output spectrum, and the $\Delta\lambda$ of the MZI spectrum and the laser output spectrum are 0.5 nm and 0.47 nm, respectively. The results show that the MZI spectrum coincides with the laser output spectrum with the same length of DCF. Thus, stable multi-wavelength lasing is obtained based on the MZI introduced by DCF. And the results also show that a multi-wavelength laser with wavelength spacing of 0.47 nm can be obtained using DCF of 0.7 m while the wavelength spacing of multi-wavelength lasing using DCF of 0.1 m is at least 3.48 nm. Because the wavelength spacings of dense wavelength division multiplexing (DWDM) system at 1.55 μm in modern communication are usually 0.8 nm and 0.4 nm, corresponding to 100 GHz and 50 GHz, respectively. Therefore, the length of DCF used in the multi-wavelength laser should be long enough to get shorter wavelength spacing suitable for the application of modern communication.

To demonstrate the influence of different lengths of DCF on pump threshold and stability, DCFs with lengths of 0.1 m and 0.7 m are used respectively. We begin this experiment using DCF of 0.1 m and continuous wave lasing starts at pump power of 40 mW. By

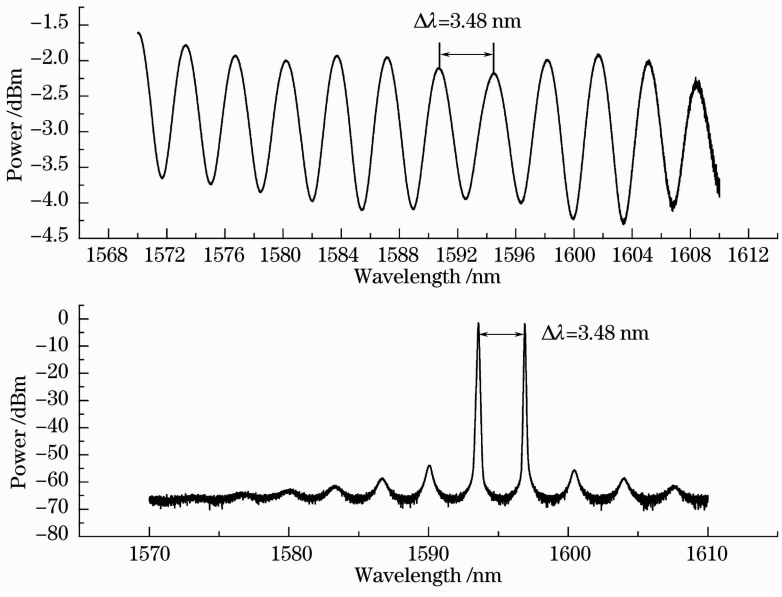

Fig. 7 MZI spectrum caused by the DCF of 0.1 m and the laser output spectrum

adjusting the PC, a different number of multi-wavelength lasing lines can be obtained. The output spectra with one-wavelength to tri-wavelength lasings are shown in Fig. 9(a) to Fig. 9(c). The signal to noise ratios (SNRs) of one-wavelength to tri-wavelength are 46, 45 and 54, respectively. The resolution and the sensitivity of OSA are set to be 0.02 nm and middle, respectively. Figure 10 shows the laser output spectrum without DCF, which is only one wavelength. It further proves that the multiwavelength output is caused by the MZI in DCF, and the DCF acts as a filter here.

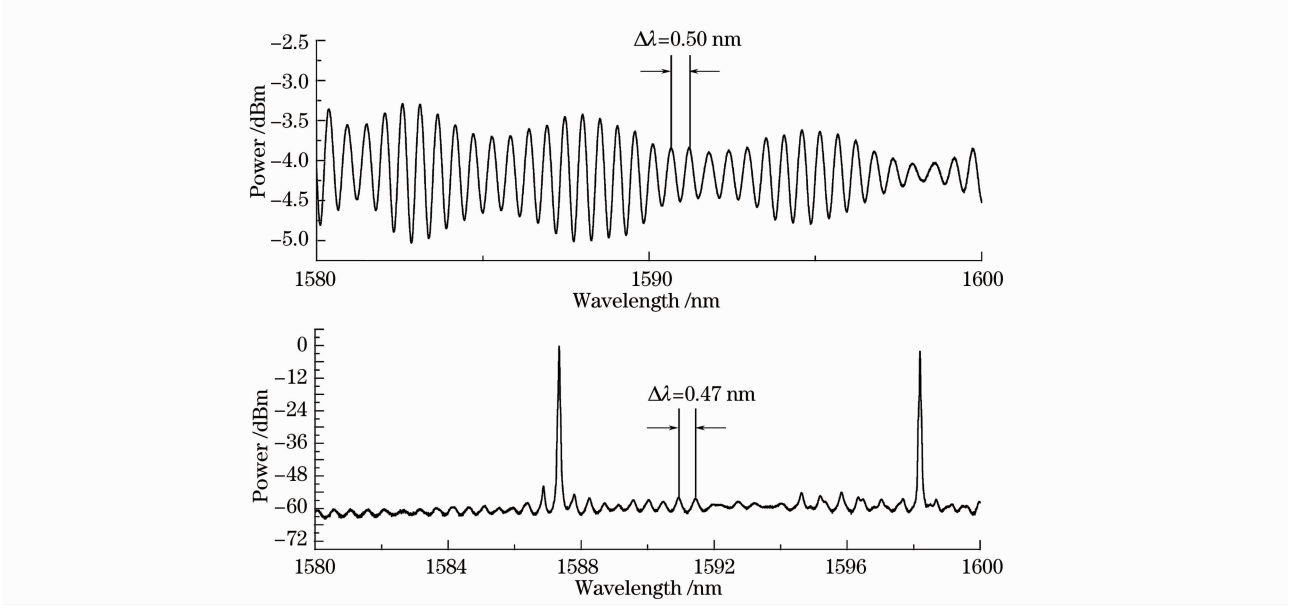

Fig. 8 MZI spectrum caused by the DCF of 0.7 m and the laser output spectrum

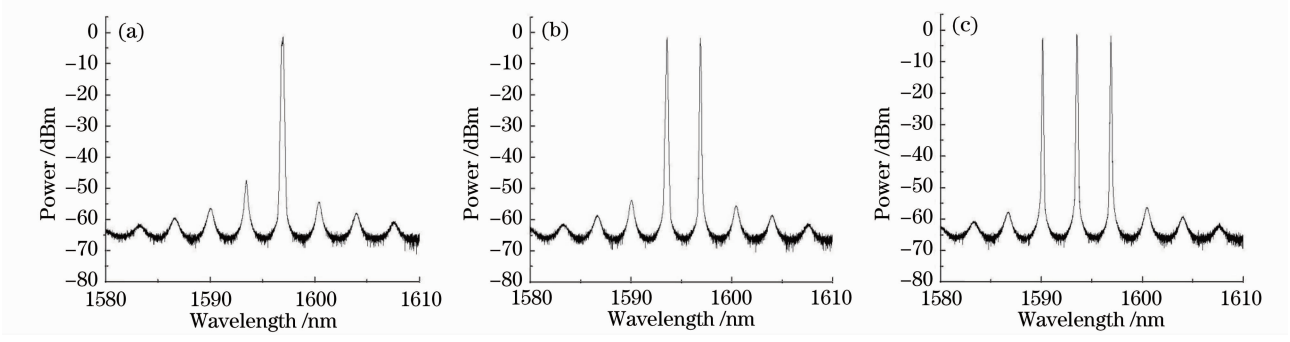

Fig. 9 Output spectra with (a) one-wavelength lasing, (b) dual-wavelength lasing and (c) tri-wavelength lasing

For the dual-wavelength and the tri-wavelength lasings, the fluctuation in output power at each wavelength is measured for five minutes, respectively. Figures 11 and 12 show the experimental results and the insert diagram shows the repeated scanning output spectra of the dual-wavelength and the tri-wavelength lasings, respectively. For the dual-wavelength lasing, the maximum power fluctuation at the wavelengths of 1593.56 nm and 1596.88 nm are about 1.08 dB and 0.77 dB, respectively, which proves the output powers are so stable. For the tri-wavelength lasing, the maximum power fluctuations at the wavelengths of 1590.19, 1593.57, 1596.96 nm are about 3.32 dB, 4.0 dB and 1.69 dB, respectively. The maximum power fluctuation of the tri-wavelength lasing is much bigger than the dual-wavelength lasing because there are more wavelengths competition so that each wavelength is affected by more factors and becomes unstable.

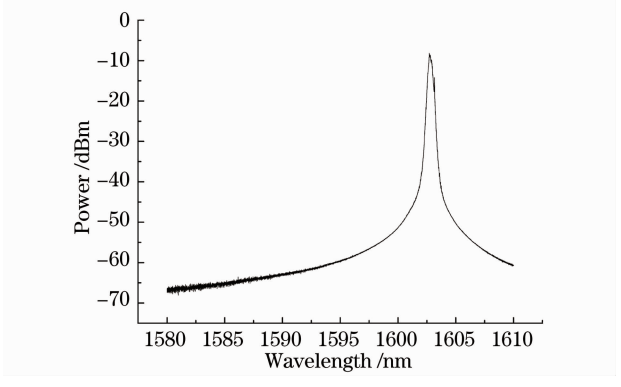

Fig. 10 Laser output spectrum without DCF

Correspondingly, DCF with length of 0.7 m is used and continuous wave lasing starts at pump power of

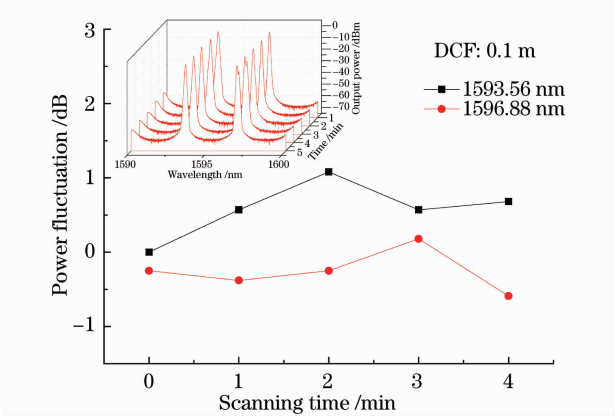

Fig. 11 Power fluctuation of the dual-wavelength lasing during scanning. Insert shows the repeated scanning output spectra of the laser

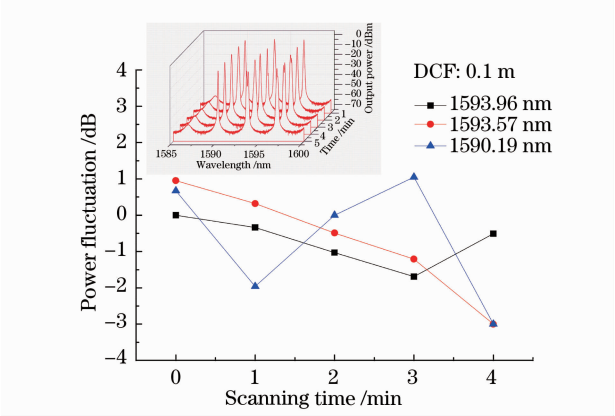

Fig. 12 Power fluctuation of the tri-wavelength lasing during scanning. Insert shows the repeated scanning output spectra of the laser

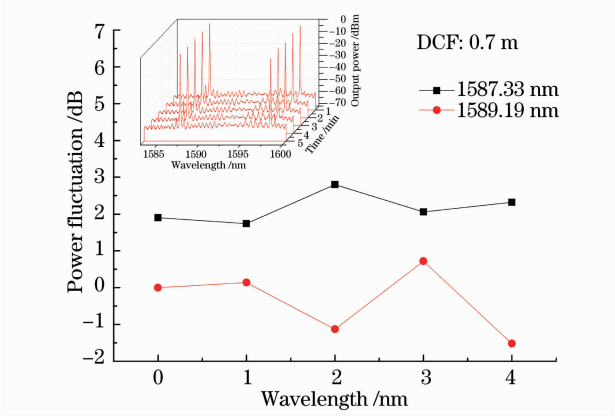

Fig. 13 Power fluctuation of the dual-wavelength lasing during scanning. Insert shows the repeated scanning output spectra of the laser

50 mW. The cavity loss increases with the length of DCF. It results in the enhancement of the pump threshold. By adjusting the PC, we can obtain a dual-wavelength lasing and its output power fluctuation is measured, the experimental results are shown in Fig. 13 and its insert diagram shows the repeated scanning output spectra. The maximum power fluctuations at the wavelengths of 1587.33 nm and 1589.19 nm are about 1.06 dB and 1.52 dB, respectively. It is higher than that using DCF of 0.1 m. Therefore, the shorter the DCF is, the more stable the multi-wavelength laser is. However, the longer the length of DCF is, the shorter wavelength spacing in the multi-wavelength laser can be obtained. Hence optimizing of the length of DCF is very important if this kind of multi-wavelength laser is applied in the DWDM system.

5 Conclusion

In conclusion, we proposed a simple approach that successfully obtains stable multi-wavelength lasing based on DCF MZI at room temperature in erbium-doped fiber ring laser. The stability of the dual-wavelength lasing is so well with peak fluctuation of 1.1 dB and much better than the tri-wavelength lasing. This kind of multi-wavelength laser has a potential application in DWDM system for its features of simple and low-cost. The length of DCF should be optimized to make the wavelength spacing and the stability of multi-wavelength laser suitable for the application of DWDM system in modern communication.

References

1 Y G Liu, X Y Dong, P Shum, *et al*.. Stable room-temperature multi-wavelength lasing realization in ordinary erbium-doped fiber loop lasers[J]. Opt Express, 2006, 14(20): 9293 - 9298.

2 H Lin. Waveband-tunable multiwavelength erbium-doped fiber laser[J]. Appl Opt, 2010, 49(14): 2653 - 2657.

3 Y G Han, C S Kim, J U Kang. Multiwavelength Raman fiber-ring laser based on tunable cascaded long-period fiber gratings[J]. IEEE Photon Technol Lett, 2003, 15(3): 383 - 385.

4 W J Zheng, S C Ruan, M Zhang, *et al*.. Switchable multi-wavelength erbium-doped photonic crystal fiber laser based on nonlinear polarization rotation[J]. Opt Laser Technol, 2013, 50: 145 - 149.

5 C L Zhao, X F Yang, C Lu, *et al*.. Switchable multi-wavelength erbium-doped fiber lasers by using cascaded fiber Bragg gratings written in high birefringence fiber[J] . Opt Commun, 2004, 230(4): 313 - 317.

6 X H Feng, H Y Tam, P K A Wai. Stable and uniform multiwavelength erbium-doped fiber laser using nonlinear polarization rotation[J]. Opt Express, 2006, 14(18): 8205 - 8210.

7 Yang Xiufeng, Peng Lei, Tong Zhengrong, *et al*.. Design of tunable bandpass photonic microwave filter based on multi-wavelength fiber laser[J]. Acta Optica Sinica, 2012, 32(2): 0206004.
杨秀峰, 彭　磊, 童峥嵘, 等. 基于多波长激光器的带通微波光子滤波器设计[J]. 光学学报, 2012, 32(2): 0206004

8 Yang Xiufeng, Fang Xiuli, Tong Zhengrong, *et al*.. Experimental study of multi-wavelength fiber laser based on phase-shifted fiber grating[J]. Chinese J Lasers, 2012, 39(6): 0602012.

杨秀峰，方秀丽，童峥嵘，等. 基于相移光栅的多波长掺铒光纤激光器的实验研究[J]. 中国激光，2012，39(6)：0602012.

9 Y G Shee, M H A Mansoori, A Ismail, *et al*.. Multiwavelength Brillouin-erbium fiber laser with double-Brillouin-frequency spacing[J]. Opt Express, 2011, 19(3): 1699 - 1706.

10 R Parvizi, S W Harun, N M Ali, *et al*.. Photonic crystal fiber-based multi-wavelength Brillouin fiber laser with dual-pass amplification configuration[J]. Chin Opt Lett, 2011, 9(2): 021403.

11 X M Liu, X Q Zhou, C Lu. Four-wave mixing assisted stability enhancement: theory, experiment, and application[J]. Opt Lett, 2005, 30(17): 2257 - 2259

12 N S Shahabuddin, Z Yusoff, H Ahmad, *et al*.. Multi-wavelength erbium-doped fiber laser using four-wave mixing effect in doped fiber[J]. Chin Opt Lett, 2011, 9(6): 061407.

13 Sun Bing, Chen Daru, Gao Shiming. Multi-wavelength fiber optical parametric oscillator with a tunable wavelength-spacing [J]. Chinese J Lasers, 2011, 38(2): 0202006.
孙 兵，陈达如，高士明. 波长间隔可调谐多波长光纤光学参量振荡器[J]. 中国激光，2011，38(2)：0202006.

14 H L An, X Z Lin, E Y B Pun, *et al*.. Multi-wavelength operation of an erbium-doped fiber ring laser using a dual-pass Mach-Zehnder comb filter[J]. Opt Commun, 1999, 169(6): 159 - 160.

15 A P Luo, Z C Luo, W C Xu. Tunable and switchable multiwavelength erbium-doped fiber ring laser based on a modified dual-pass Mach-Zehnder interferometer[J]. Opt Lett, 2009, 34(14): 2135 - 2137.

16 C He, X L Zeng, F F Pang, *et al*.. Switchable multi-wavelength fiber laser using in-fiber Mach-Zehnder interferometer[J]. 15th Optoelectronics and Communications Conference (OECC2010) Technical Digest, 2010, 7P(51): 358 - 359.

17 M Shtaif, C R Menyuk, M L Dennis, *et al*.. Carrier-envelope phase locking of multi-pulse lasers with an intra-cavity Mach-Zehnder interferometer[J]. Opt Express, 2011, 19(23): 23202 - 23214.

18 B Dong, L Wei, D P Zhou. Miniature high-sensitivity high-temperature fiber sensor with a dispersion compensation fiber-based interferometer[J]. Appl Opt, 2009, 48(33): 6466 - 6469.

栏目编辑：王晓琰